## PROCEEDINGS OF SPIE

SPIEDigitalLibrary.org/conference-proceedings-of-spie

# Demonstration of a photonic-lantern focal-plane wavefront sensor using fiber mode conversion and deep learning

Barnaby R. Norris, Jin Wei, Christopher Betters, Sergio Leon-Saval, Yinzi Xin, et al.

Barnaby R. M. Norris, Jin Wei, Christopher H. Betters, Sergio G. Leon-Saval, Yinzi Xin, Jonathan Lin, Yoo Jung Kim, Steph Sallum, Julien Lozi, Sebastien Vievard, Olivier Guyon, Pradip Gatkine, Nemanja Jovanovic, Dimitri Mawet, Michael P. Fitzgerald, "Demonstration of a photonic-lantern focal-plane wavefront sensor using fiber mode conversion and deep learning," Proc. SPIE 12185, Adaptive Optics Systems VIII, 1218530 (29 August 2022); doi: 10.1117/12.2629852



Event: SPIE Astronomical Telescopes + Instrumentation, 2022, Montréal, Québec, Canada

### Demonstration of a photonic-lantern focal-plane wavefront sensor using fiber mode conversion and deep learning

Barnaby R. M. Norris<sup>a,b,c</sup>, Jin Wei<sup>a,b,c</sup>, Christopher H. Betters<sup>a,b,c</sup>, Sergio G. Leon-Saval<sup>a,b,c</sup>, Yinzi Xin<sup>d</sup>, Jonathan Lin<sup>e</sup>, Yoo Jung Kim<sup>e</sup>, Steph Sallum<sup>f</sup>, Julien Lozi<sup>g</sup>, Sebastien Vievard<sup>g</sup>, Olivier Guyon<sup>g</sup>, Pradip Gatkine<sup>d</sup>, Nemanja Jovanovic<sup>d</sup>, Dimitri Mawet<sup>d</sup>, and Michael P. Fitzgerald<sup>e</sup>

<sup>a</sup>Sydney Institute for Astronomy, School of Physics, University of Sydney, NSW 2006, Australia

<sup>b</sup>Sydney Astrophotonic Instrumentation Laboratories, School of Physics, University of Sydney, NSW 2006, Australia

<sup>c</sup>Astralis, Astronomical Instrumentation Consortium, Australia <sup>d</sup>Department of Astronomy, California Institute of Technology, 1200 E. California Blvd, Pasadena, USA

<sup>e</sup>Physics & Astronomy Department, University of California, Los Angeles (UCLA), 475 Portola Plaza, Los Angeles, USA

<sup>f</sup>Department of Physics & Astronomy, University of California, Irvine, 4129 Frederick Reines Hall, Irvine, CA 92697 USA

<sup>g</sup>Subaru Telescope, National Astronomical Observatory of Japan, National Institutes of Natural Sciences (NINS), 650 North A'ohōkū Place, Hilo, HI 96720, United States

#### ABSTRACT

A focal plane wavefront sensor offers major advantages to adaptive optics, including removal of non-common-path error and providing sensitivity to blind modes (such as petalling). But simply using the observed point spread function (PSF) is not sufficient for wavefront correction, as only the intensity, not phase, is measured. Here we demonstrate the use of a multimode fiber mode converter (photonic lantern) to directly measure the wavefront phase and amplitude at the focal plane. Starlight is injected into a multimode fiber at the image plane, with the combination of modes excited within the fiber a function of the phase and amplitude of the incident wavefront. The fiber undergoes an adiabatic transition into a set of multiple, single-mode outputs, such that the distribution of intensities between them encodes the incident wavefront. The mapping (which may be strongly non-linear) between spatial modes in the PSF and the outputs is stable but must be learned. This is done by a deep neural network, trained by applying random combinations of spatial modes to the deformable mirror. Once trained, the neural network can instantaneously predict the incident wavefront for any set of output intensities. We demonstrate the successful reconstruction of wavefronts produced in the laboratory with low-wind-effect, and an on-sky demonstration of reconstruction of low-order modes consistent with those measured by the existing pyramid wavefront sensor, using SCExAO observations at the Subaru Telescope.

**Keywords:** photonic lantern, astrophotonics, focal plane wavefront sensor, machine learning, photonic wavefront sensor, fiber injection

#### 1. INTRODUCTION

In recent years photonics have revolutionised astronomical instrumentation, due to their precision, their compact and stable form factor, and capability to perform complicated optical processing. Here we describe the use of

Further author information: (Send correspondence to B.N.)

B.N.: E-mail: barnaby.norris@sydney.edu.au

Adaptive Optics Systems VIII, edited by Laura Schreiber, Dirk Schmidt, Elise Vernet, Proc. of SPIE Vol. 12185, 1218530 ⋅ © 2022 SPIE 0277-786X ⋅ doi: 10.1117/12.2629852

a photonic mode-converter device – the photonic lantern (PL) – as a focal plane wavefront sensor and related applications.

A focal plane wavefront sensor in general is highly sought after in adaptive optics (AO) for various reasons, including it being sensitive to blind modes such as low-wind-effect or petalling, and it being at the same optical plane and wavelength as the science image thus avoiding non-common-path aberrations.

In particular, low wind effect (also petalling, island modes, hereafter collectively referred to as LWE)<sup>1-4</sup> is currently a major limitation in high angular resolution AO and so methods to correct it are urgently required. This effect occurs when phase discontinuities across the telescope's secondary-mirror supports (spiders) form, exacerbated by thermal effects (especially in low wind conditions). This phase shear results in a severely broken-up PSF. But conventional pupil-plane wavefront sensors (such as pyramid and Shack-Hartmann wavefront sensors) are insensitive to this effect. This effect is, however, clearly measurable in the focal plane.

Simply using the focal plane image as a wavefront sensor (WFS) is not possible since intensity alone contains an ambiguity as to the sign of an aberration. Hence a method to measure both the phase and amplitude of the electric field at the focal plane is required. Various approaches have been proposed;<sup>5–9</sup> these often use a linear approximation (i.e. wavefront error (WFE)  $\lesssim 1$  rad, which may not be the case with LWE), require iterative processing precluding real-time use, require active deformable mirror (DM) modulation or require modifications to the visible pupil.

Using a photonic lantern as a focal plane wavefront sensor  $^{10-12}$  offers several advantages over conventional wavefront sensors:

- The direct measurement of the *complex* amplitude at the focal plane, and sensitivity to blind-modes such as LWE
- It features optimal use of detector pixels (and hence minimisation of read/dark noise) just one pixel per mode sensed
- It is ideal for truly zero-non-common-path high-throughout injection into single-mode fibers, with wavefront sensor and science fiber in one device
- It is straightforward to spectrally disperse, allowing multi-wavelength wavefront sensing to unwrap phase, sense scintillation, etc.
- The entire device fits within a standard optical fiber connector (e.g. FC/PC or SMA), making deployment in existing systems simple, and well suited to multi-object sensing
- The PSF can simultaneously be measured, and there is a path to full complex imaging as number of modes increases

#### 2. THE PHOTONIC LANTERN AS WAVEFRONT SENSOR

A photonic lantern<sup>13–15</sup> (PL) is a photonic device which converts the light in a multimode fiber into multiple, single-mode (SM) fibers with high efficiency. To do this adiabatically, the number of output SM fibers must equal (or exceed) the number of modes present in the multimode input.

This is achieved by way of a carefully engineered taper transition, wherein the cores of the SM fibers disappear and their cladding becomes the core of the new multimode fiber, the cladding of which is a low refractive index capillary. These devices can be manufactured by placing multiple individual SM fibers into a capillary and performing the taper, though more recently multi-core fibers (MCF) have been used. <sup>16</sup> Here, an MCF containing multiple separated single-mode cores is used instead of multiple bulk fibers, simplifying the process and easily allowing devices with many more modes/cores to be produced.

In a standard PL, there is not a one-to-one mapping between input mode and output fiber. Rather the *complex* output of each fiber is a linear combination of the complex amplitudes of each input mode. Figure 1 shows such a transfer matrix for a 19 core, 19 mode device operating at 1550 nm modelled using RSoft. Note that while this matrix can be obtained from a modelled device, it is not generally possible to obtain this complex

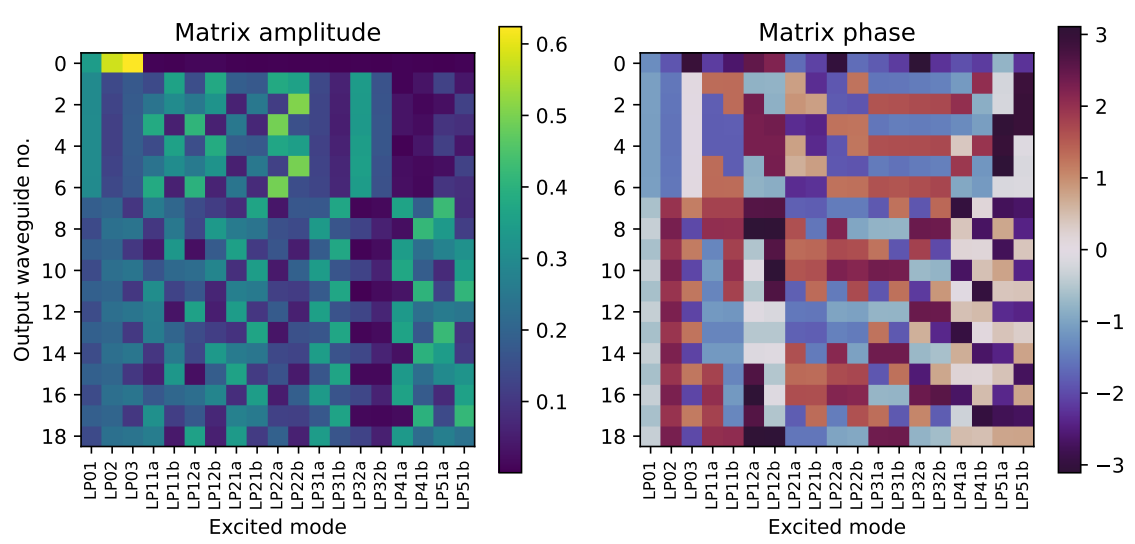


Figure 1: The complex coupling matrix for a 19 mode photonic lantern from an RSoft model. The complex output of each SM waveguide (or SM fiber) is a linear combination of the complex amplitudes of the input modes. In practice, the output *intensities* (the square of the amplitudes) are measured, making the device's transfer function nonlinear. This particular PL was designed as a multicore-fiber type and optimised for a wavelength of 1550 nm. Amplitudes are normalised with each input mode having amplitude of 1, and phases are in radians.

matrix for a physical device. In practice the intensity (which is the square of the complex amplitude) of the output fibers are measured, meaning that the relationship between the quantity of interest (wavefront phase) and the measured quantity is nonlinear.<sup>10,17</sup>

The key to the wavefront sensing application is that the excitation of the various modes in a multimode fiber is a direct function of the spatially dependent complex amplitude of the light being injected into it. Thus when placed at the focal plane, the modal content of the fiber encodes the complex PSF. If the complex amplitude of each mode could be measured then the focal plane wavefront could be inferred. Directly measuring the modal coefficients for a multimode fiber, such as imaging its output mode-field and fitting calculated mode patterns, is not practical outside of a laboratory setting - it is computationally slow and cannot be performed in realtime, requires high resolution imaging and thus is badly impacted by read noise, and is unstable. Instead, a photonic lantern is used. If the transfer function is known then the wavefront can be determined simply by measuring the intensities of the SM output fibers. The broad properties of a given PL as defined by its geometric and material properties can be modelled using numerical techniques such as BPM, and the general relationship of design parameters to the device's transfer function can be analysed.<sup>18</sup>

However, the exact transfer function of a PL cannot be precisely specified at design time. But, once it is manufactured this function is very stable. To ensure this, in practice the telescope PSF is directly imaged onto the short, multimode region of the PL, rather than using a connecting multimode fiber, ensuring no changes in strain or temperature can affect the mapping. Thus the transfer function must be learned in situ. Since the transfer function from input phase / amplitude to output intensity is non-linear, several approaches can be used.

One method is to use a machine-learning algorithm well suited to non-linearities, such as a neural network (NN).<sup>10</sup> In this case a set of training data, produced by injecting random (but known) combinations of input wavefronts and measuring the output intensities, is used to train a neural network model which learns the devices transfer function. Once trained, the NN is used much a like a control matrix in standard AO – the measured PL output intensities are input and the corresponding wavefront phase is output. A key aspect of this method is that all training data can be produced in-situ in a standard AO system, needing no equipment beyond the system's existing light source and deformable mirror. Further information on the PL WFS's nonlinearity and the corresponding use of a NN are detailed in Wong, et al. (2022).<sup>17</sup>

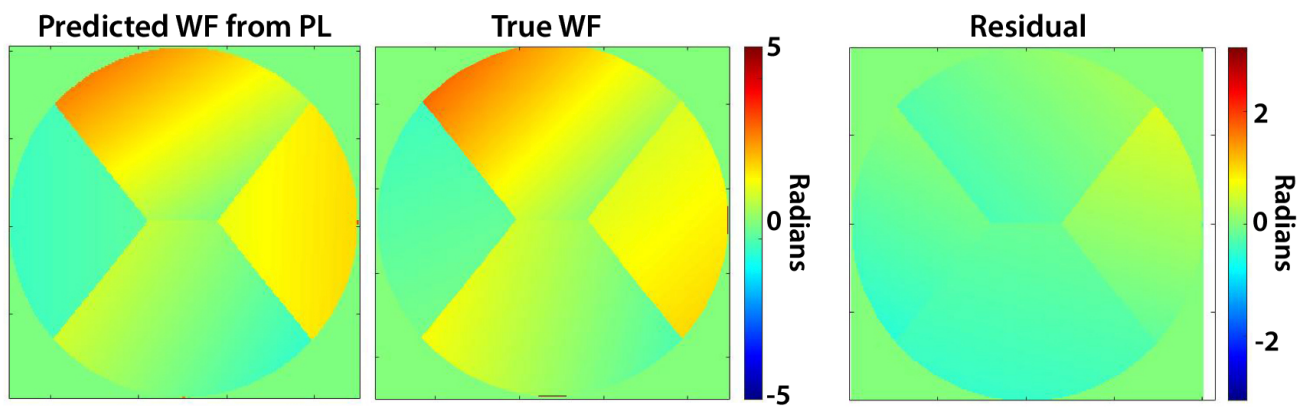


Figure 2: Result of laboratory test of the ability of the PL WFS to sense and reconstruct low wind effect modes. The left panel shows the wavefront reconstructed by the PL WFS, and the middle panel shows the true wavefront applied (via an SLM). The magnitude of this wavefront error is large, with P-V of  $\sim$ 10 radians. The right panel shows the residual between reconstructed and true wavefront - note the smaller values on the colour bar.

Another approach is to restrict operation to wavefronts with smaller phase errors, and linearise the problem. <sup>19</sup> This has the key advantage that it is directly compatible with existing linear AO control systems. Alternatively, some type of analytic second-order (or higher) reconstruction could be performed. <sup>19</sup> In the examples shown in this paper, the neural network method was used.

#### 3. WAVEFRONT SENSING RESULTS

Several experiments, both in the lab and on-sky, were performed to evaluate the use of a PL as a wavefront sensor. Previously  $^{10}$  a laboratory experiment demonstrated the performance of a PL to reconstruct the first 9 Zernike modes of a wavefront, and was able to successfully reconstruct the Zernike coefficients for incident wavefronts of  $\sim \pi$  radians P-V to an accuracy of  $1.6 \times 10^{-2}$  radians RMS. In this case the NN learned the PL's transfer function from  $\sim 50~000$  examples of random wavefronts (composed of randomly chosen Zernike coefficients) applied to the system's spatial light modulator (SLM), and its success evaluated on  $\sim 10~000$  previously unseen examples (to detect model overfitting). This training data would take  $\sim 30$  seconds to acquire on a modern AO system running at KHz speeds.

In a similar experiment, the ability of the PL WFS to sense and reconstruct LWE (petalling) modes was evaluated. Figure 2 shows an example of a LWE wavefront successfully reconstructed in the laboratory test, using a 19 core MCF PL. The LWE wavefront was parameterised by each of the 4 pupil segments having a tip, tilt and piston value. The test wavefront shown has a P-V amplitude of  $\sim$ 10 radians, well beyond the linear regime. Training data was acquired as per the experiment described above, but now using these LWE coefficients instead of Zernike coefficients.

An on-sky test, using the SCExAO system at the Subaru telescope, was also performed. Unlike in the laboratory, where known test wavefronts are applied to the SLM and the accuracy of the PL WFS's ability to reconstruct them is evaluated, on-sky there is no known 'true' wavefront. Instead, the accuracy of the PL WFS in matching the low-order modes detected by the system's existing pyramid WFS was evaluated. A 19 mode PL was used, and the lowest 19 modes measured by SCExAO's existing wavefront reconstruction (from the pyramid WFS) were used as the 'truth' data (i.e. for training and evaluation). This is not an optimal test, since the pyramid WFS is insensitive to blind modes (such as LWE) and the reconstruction is linearised, hence this test can not demonstrate the ability of the PL WFS to detect these features. Nonetheless it is a useful baseline comparison. Figure 3 shows an example of a low-order wavefront reconstructed by the PL WFS from on-sky observations of Vega, performed by SCExAO in March 2022, demonstrating the successful reconstruction of a wavefront.

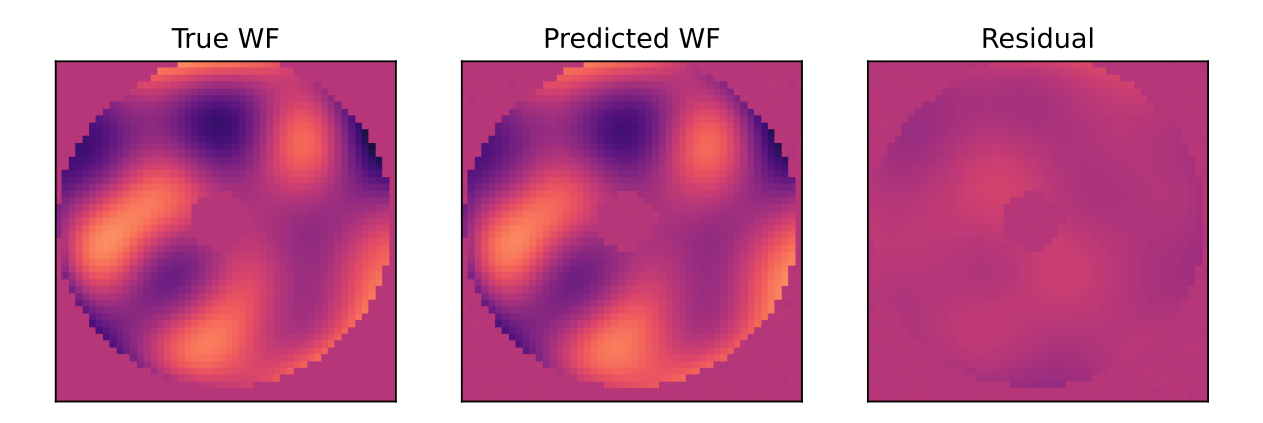


Figure 3: Result of an on-sky test of the ability of the PL WFS to sense and reconstruct low order wavefronts, from SCExAO / Subaru Telescope observations of Vega in March 2022. Here, the lowest 19 modes sensed by the existing pyramid WFS (and its linear reconstructor) are used as the 'truth' comparison. It can be seen that the PL WFS reconstructs the same wavefront as the pyramid WFS with low residuals. See text for details.

#### 4. CONCLUSION AND NEXT STEPS

The photonic lantern wavefront sensor allows direct measurement of the phase and amplitude of the PSF, which is encoded in the output intensities of a set of single-mode fibers. It is sensitive to modes which pupil-plane wavefront sensors can not easily detect (such as low wind effect / petalling), is ideal for applications which require injection into single mode fibers (having zero non-common-path aberrations), makes optimal use of detector pixels (one pixel per mode), is simple to spectrally disperse for multi-wavelength wavefront sensing and is extremely compact, fitting into a standard fiber connector.

The ability of this device to accurately measure wavefronts has been demonstrated in the lab and in preliminary on-sky tests. Further, detailed on-sky testing of wavefront sensing and also PSF reconstruction is ongoing, and publication of comprehensive results is forthcoming.

Using the PL WFS in closed loop for adaptive optics is the clear next step, and requires new algorithms to be implemented into the existing AO control systems. These may be neural-network based (as used in this paper), linearised reconstructors if wavefront errors are small or some other type of nonlinear model.

Current demonstration devices have a small number of modes (19 in this case), but scaling to large numbers of modes is straightforward, with PLs having 100s of modes already having been designed.<sup>20</sup> Not only will this allow higher order wavefront errors to be measured, but it will also enable complete, combined imaging and wavefront sensing in a single unit. In addition to wavefront sensing and imaging, it is also optimal for high efficiency injection into a SM fiber for astrophotonic instruments (such as single-mode spectrographs), for use with nulling methods such as the Vortex Fiber Nuller<sup>21</sup> and spectroastrometry.<sup>22</sup> The range of applications of photonic lanterns in astronomy is rapidly expanding, with ongoing development enabling new photonic sensing and processing capabilities in the coming years.

#### REFERENCES

[1] Sauvage, J.-F., Fusco, T., Lamb, M., Girard, J., Brinkmann, M., Guesalaga, A., Wizinowich, P., O'Neal, J., N'Diaye, M., Vigan, A., Mouillet, D., Beuzit, J.-L., Kasper, M., Le Louarn, M., Milli, J., Dohlen, K., Neichel, B., Bourget, P., Haguenauer, P., and Mawet, D., [Tackling down the low wind effect on SPHERE instrument], vol. 9909 of Society of Photo-Optical Instrumentation Engineers (SPIE) Conference Series, 990916 (2016).

- [2] Milli, J., Kasper, M., Bourget, P., Pannetier, C., Mouillet, D., Sauvage, J. F., Reyes, C., Fusco, T., Cantalloube, F., Tristam, K., Wahhaj, Z., Beuzit, J. L., Girard, J. H., Mawet, D., Telle, A., Vigan, A., and N'Diaye, M., "Low wind effect on VLT/SPHERE: impact, mitigation strategy, and results," in [Proceedings of the SPIE], Society of Photo-Optical Instrumentation Engineers (SPIE) Conference Series 10703, 107032A (Jul 2018).
- [3] N'Diaye, M., Martinache, F., Jovanovic, N., Lozi, J., Guyon, O., Norris, B., Ceau, A., and Mary, D., "Calibration of the island effect: Experimental validation of closed-loop focal plane wavefront control on Subaru/SCExAO," Astronomy and Astrophysics 610, A18 (Feb. 2018).
- [4] Vievard, S., Bos, S., Cassaing, F., Ceau, A., Guyon, O., Jovanovic, N., Keller, C. U., Lozi, J., Martinache, F., Montmerle-Bonnefois, A., Mugnier, L., NDiaye, M., Norris, B., Sahoo, A., Sauvage, J.-F., Snik, F., Wilby, M. J., and Wong, A., "Overview of focal plane wavefront sensors to correct for the Low Wind Effect on SUBARU/SCExAO," arXiv e-prints, arXiv:1912.10179 (Dec 2019).
- [5] Mocœur, I., Mugnier, L. M., and Cassaing, F., "Analytical solution to the phase-diversity problem for real-time wavefront sensing," *Opt. Lett.* **34**, 3487–3489 (Nov 2009).
- [6] Vievard, S., Cassaing, F., Mugnier, L. M., Bonnefois, A., and Montri, J., "Real-time full alignment and phasing of multiple-aperture imagers using focal-plane sensors on unresolved objects," SPIE 10698, 106986F (July 2018).
- [7] Korkiakoski, V., Keller, C. U., Doelman, N., Kenworthy, M., Otten, G., and Verhaegen, M., "Fast & Eurious focal-plane wavefront sensing," *Applied Optics* **53**(20), 4565 (2014).
- [8] Martinache, F., "The Asymmetric Pupil Fourier Wavefront Sensor," PASP 125, 422 (Apr 2013).
- [9] Martinache, F., Guyon, O., Jovanovic, N., Clergeon, C., Singh, G., Kudo, T., Currie, T., Thalmann, C., McElwain, M., and Tamura, M., "On-Sky Speckle Nulling Demonstration at Small Angular Separation with SCExAO," PASP 126, 565 (Jun 2014).
- [10] Norris, B. R. M., Wei, J., Betters, C. H., Wong, A., and Leon-Saval, S. G., "An all-photonic focal-plane wavefront sensor," *Nature Communications* 11, 5335 (Oct. 2020).
- [11] Corrigan, M. K., Morris, T. J., Harris, R. J., and Anagnos, T., "Demonstration of a photonic lantern low order wavefront sensor using an adaptive optics testbed," in [Adaptive Optics Systems VI], Close, L. M., Schreiber, L., and Schmidt, D., eds., 10703, 1313 1320, International Society for Optics and Photonics, SPIE (2018).
- [12] Cruz-Delgado, D., Alvarado-Zacarias, J. C., Cooper, M. A., Wittek, S., Dobias, C., Martinez-Mercado, J., Antonio-Lopez, J. E., Fontaine, N. K., and Amezcua-Correa, R., "Photonic lantern tip/tilt detector for adaptive optics systems," Opt. Lett. 46, 3292–3295 (Jul 2021).
- [13] Leon-Saval, S. G., Birks, T. A., Bland-Hawthorn, J., and Englund, M., "Multimode fiber devices with single-mode performance," *Optics Letters* **30**, 2545–2547 (Oct 2005).
- [14] Leon-Saval, S. G., Argyros, A., and Bland -Hawthorn, J., "Photonic lanterns," Nanophotonics 2, 429–440 (Dec 2013).
- [15] Birks, T. A., Gris-Sánchez, I., Yerolatsitis, S., Leon-Saval, S. G., and Thomson, R. R., "The photonic lantern," Advances in Optics and Photonics 7, 107 (Jun 2015).
- [16] Birks, T. A., Mangan, B. J., Díez, A., Cruz, J. L., and Murphy, D. F., "Photonic lantern" spectral filters in multi-core Fiber," *Optics Express* **20**, 13996 (Jun 2012).
- [17] Wong, A. et al., "Machine learning for wavefront sensing," These proceedings, Paper 12185-90 (2022).
- [18] Lin, J., Jovanovic, N., and Fitzgerald, M. P., "Design considerations of photonic lanterns for diffraction-limited spectrometry," *Journal of the Optical Society of America B Optical Physics* 38, A51 (July 2021).
- [19] Lin, J. et al., "Exoplanet detection with photonic lanterns for focal-plane wavefront sensing and control," These proceedings, Paper 12185-88 (2022).
- [20] Leon-Saval, S. G., Betters, C. H., Salazar-Gil, J. R., Min, S.-S., Gris-Sanchez, I. e., Birks, T. A., Lawrence, J., Haynes, R., Haynes, D., Roth, M., Veilleux, S., and Bland -Hawthorn, J., "Divide and conquer: an efficient solution to highly multimoded photonic lanterns from multicore fibres," Optics Express 25, 17530 (Jul 2017).
- [21] Xin, Y. et al., "Efficient detection and characterization of exoplanets within the diffraction limit: vortex fiber nulling with a mode-selective photonic lantern," In preparation (2022).
- [22] Kim, Y. J. et al., "Spectroastrometry with photonic lanterns," These proceedings, Paper 12184-158 (2022).